Sr, Nd, and Pb isotope evidence for a mantle origin of alkali chlorides and carbonates in the Udachnaya kimberlite, Siberia

Roland Maas   School of Earth Sciences, University of Melbourne, Parkville, Victoria 3010, Australia, and Max-Planck Institut für Chemie, Mainz 55020, Germany

Maya B. Kamenetsky*   Centre for Ore Deposit Research, University of Tasmania, Hobart, Tasmania 7001, Australia, and Max-Planck Institut für Chemie, Mainz 55020, Germany

Alexander V. Sobolev   Max-Planck Institut für Chemie, Mainz 55020, Germany, and Vernadsky Institute of Geochemistry, Moscow 117975, Russia

Vadim S. Kamenetsky   Centre for Ore Deposit Research, University of Tasmania, Hobart, Tasmania 7001, Australia, and Max-Planck Institut für Chemie, Mainz 55020, Germany

Nikolai V. Sobolev   Institute of Mineralogy and Petrography, Novosibirsk 630090, Russia

ABSTRACT

The kimberlite rocks of the Udachnaya-East pipe (Siberia) are uniquely fresh and contain very high abundances of primary volatiles (Cl, CO_2, S). Alkali elements and chlorine are extremely abundant in the reconstructed kimberlite melt compositions, and this enrichment is very important for our understanding of deep-mantle melting and melt transport. Here we present new isotopic data that confirm a mantle origin for these kimberlitic chlorides and carbonates, and constrain the kimberlite emplacement age as ca. 347 Ma. The initial Nd and Pb isotope ratios in a large salt aggregate, in a Cl-S–enriched water leachate of the groundmass, and in the silicate fraction of the groundmass are very similar ($\varepsilon_{Nd} = +3$ to $+4$, $^{206}Pb/^{204}Pb = 18.6$, $^{207}Pb/^{204}Pb = 15.53$), implying a comagmatic origin of the chlorides and carbonates and the silicates. Combined Sr, Nd, and Pb isotope data are used to rule out any significant contributions to the kimberlite chlorine budget from crustal sources, such as the Cambrian evaporite sequences of the Siberian platform. Our data support the interpretation that exsolved Na-K chloride and Na-K-Ca carbonate formed directly from original uncontaminated kimberlite magma. High Cl abundances in kimberlites suggest the presence of a Cl-rich reservoir in the deep sublithospheric mantle.

Keywords: kimberlite, radiogenic isotopes, volatiles, chlorine, carbonate, mantle.

INTRODUCTION

The parent magmas of kimberlites, the principal source of diamonds, originate from mantle depths of 150–200 km, deeper than any other known terrestrial magma (e.g., Dawson, 1980; Haggerty, 1999; Mitchell, 1989). Although much progress has been made in understanding their origin (e.g., Harris et al., 2004; le Roex et al., 2003; Price et al., 2000; Rao et al., 2004), many aspects of the composition and genesis of primary kimberlite magmas are still unclear. One key issue is the nature of volatiles in the mantle and kimberlite magmas and their role in partial melting, melt extraction, and transport from deep-mantle source regions. Other questions relate to the effects of different volatiles on diamond nucleation and growth (e.g., Pal'yanov et al., 2002; Tomlinson et al., 2004).

The presence of chlorides in some Siberian kimberlites has been previously attributed to postmagmatic interaction with saline groundwaters (e.g., Pavlov and Ilupin, 1973). Kamenetsky et al. (2004) presented the first petrographic, chemical, and melt inclusion evidence for primary magmatic origin of water-soluble alkali chlorides, carbonates, and sulfates in the Udachnaya-East kimberlite (Yakutia, Siberia). The preservation of a mantle-derived volatile signature in these kimberlites is thought to be linked to the absence of synmagmatic and postmagmatic alteration (Golovin et al., 2003; Kamenetsky et al., 2004), alteration being an otherwise common feature in most other kimberlites (Mitchell, 1986). If confirmed, the discovery of a Cl-rich component in kimberlite mantle sources would represent an important advance in our understanding of deep-mantle melting and kimberlite petrogenesis.

In this paper we address the issue of crustal contamination as a source of Cl-rich components in the Udachnaya kimberlite. Like most Yakutian kimberlites, the Udachnaya pipes were emplaced through Cambrian carbonates and evaporites. Furthermore, pools of Mg-Na-Cl–rich brine derived from sedimentary rocks are present in the Udachnaya open pit. A crustal source of some or all of the Cl-rich material in the kimberlite groundmass thus appears feasible and would seriously weaken the conclusions of Kamenetsky et al. (2004).

However, new Sr, Nd, and Pb isotope data for sequential leachates of the kimberlite groundmass samples rule out a crustal origin and confirm a primary mantle origin for the alkali chloride-carbonate components in this kimberlite. The data also provide new constraints on the emplacement age of the Udachnaya-East pipe.

SAMPLE DESCRIPTION

The Udachnaya kimberlite, one of numerous diamond-bearing Devonian–Carboniferous kimberlites in Yakutia, consists of two intersecting pipes (East and West) emplaced in Ordovician limestones and dolomites. Perovskite U-Pb dating indicates an age range of 367–353 Ma (Griffin et al., 1999; Kinny et al., 1997). Kimberlites in this area erupted through thick Vendian–Cambrian platform carbonate-evaporite sequences overlying Archean–Proterozoic basement of the Siberian craton (Pelechaty et al., 1996; Sobolev, 1984). The samples studied here and described in Kamenetsky et al. (2004) are from the lower part (~500 m) of the Udachnaya-East open pit and are practically unaltered. Groundmass comprises euhedral silicates (olivine, phlogopite, monticellite, plagioclase, sodalite), oxides (perovskite, spinel, titanomagnetite), sulfides (pyrrhotite, djerfisherite), Na-K chlorides, Na-Ca sulfates, apatite, and calcite; serpentinite is absent. Losses on ignition (LOI) of as much as 17% are related to abundant chlorides and carbonates volatile at 1000 °C. Groundmass samples show chemical features (Table DR1)[1] typical of kimberlites, although alkalies (3.5–5.1 wt% Na_2O, 1.9–2.2 wt% K_2O) and Cl (2.2–3.1 wt%) are unusually high. Trace element patterns (Fig. 1) show the characteristi-
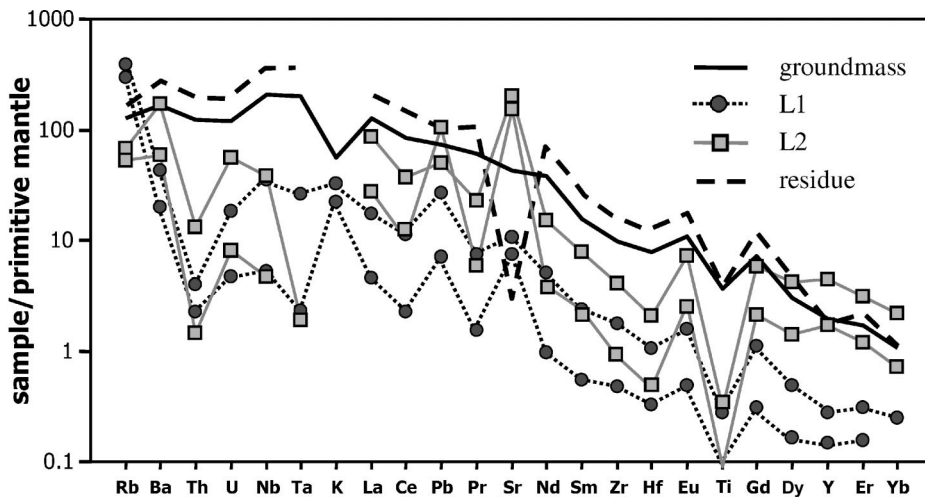
Figure 1. Primitive-mantle–normalized (Sun and McDonough, 1989) multi-element diagram showing patterns for average unleached groundmass, average HCl residues (only average patterns shown), water (L1), and HCl leachates (L2) (Table DR1; see footnote 1 in text). Unleached groundmass shows patterns typical of kimberlites; pattern for HCl residue is subparallel to unleached groundmass (no data for K in residues and L2 fractions). Cl-rich water leachates (L1) have much lower trace element levels with notable anomalies for Rb and K. HCl leachates (L2), representing carbonate component, show greater compositional extremes than L1, notably for Sr.

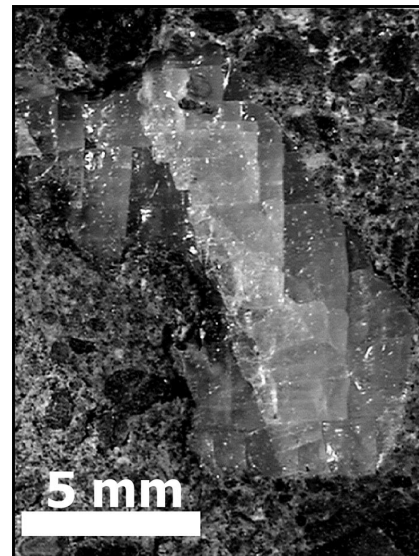Figure 2. Aggregate of chloride crystals set in microcrystalline kimberlite matrix. Sample donated by V. Sharygin.

cally strong enrichment in most incompatible trace elements and strong rare earth element (REE) fractionation.

RESULTS

In an attempt to extract Cl- and CO_3-rich groundmass components of purported mantle origin (Kamenetsky et al., 2004), two representative samples (YBK-0, YBK-3) were leached sequentially with cold distilled water (L1, L1*) and cold 1M HCl (L2), leaving a silicate-rich residue. Isotopic data were also obtained for a large salt aggregate in YBK-3 (Fig. 2). Appendix DR1 (see footnote 1) provides details of analytical procedures and chemical data.

Water leachates of the groundmass (L1, 7.3–10.8 wt% of original bulk samples) removed a component enriched in alkalies, Cl, carbonate, and sulfate (Table DR1; see footnote 1). Overall trace element levels of L1 are low (Fig. 1); in detail, contents of large ion lithophile elements are high relative to high field strength elements and Th. Rubidium appears to be anomalously high. Further leaching with dilute HCl (L2) produced mass losses of 24–32 wt% (Table DR1). Lively CO_2 degassing suggests that a carbonate component (calcite) was principally dissolved. Trace element patterns of L2 resemble those for the L1 fractions but show greater extremes, most notably for Sr (Fig. 1). Unlike HCl leachates from some other kimberlites (e.g., Alibert and Albarède, 1988), those produced here have low REE contents. As expected, the residues have broadly complementary trace element patterns (Fig. 1). Overall, leaching had only

minor effects on bulk trace element budgets, which explains the similarity of the residue and bulk groundmass patterns.

The L1 fractions have moderate Rb/Sr ratios, as well as low U/Pb and Sm/Nd ratios; the measured $^{87}Sr/^{86}Sr$ is ~0.707 (Table 1). The L2 fractions contain the bulk of the Sr but only minor proportions of the Nd and Pb; Rb/Sr and U-Th/Pb ratios are low, consistent with the trace element patterns. Measured $^{87}Sr/^{86}Sr$ ratios (0.7049–0.7059) are lower than those in L1. The residues have complementary Rb-Sr and U-Pb elemental and isotopic signatures.

Initial $^{87}Sr/^{86}Sr$ (at 367 Ma, <0.700, Table 1) in the L1 fractions are unrealistic, possibly owing to excessive release of Rb into the water solution (Fig. 1), producing spurious age corrections. However, initial ε_{Nd} values for L1*, the two L2 fractions, the HCl residues, and the unleached groundmass samples are comparable ($\varepsilon_{Nd} \approx +4$). In detail, minor isotopic disequilibrium is apparent between the leachates (L1*, L2) and the respective residues; the latter have very low $^{87}Sr/^{86}Sr$ ratios (<0.7037) relative to their ε_{Nd} values. Residue-leachate Pb isotope disequilibrium is observed for YBK-0 but not for YBK-3. Initial Pb isotope ratios for the salt aggregate (Fig. 2; age correction was minimal because of very low U and Pb) are within the range shown by the groundmass fractions (Table 1).

Initial isotope ratios for the two unleached groundmass samples ($^{87}Sr/^{86}Sr \approx 0.7047$, $\varepsilon_{Nd} \approx +4$, $^{206}Pb/^{204}Pb \approx 18.7$, $^{207}Pb/^{204}Pb = 15.53$, $^{208}Pb/^{204}Pb = 37.5–38.6$, $t = 367$ Ma; Table 1) are comparable to Sr-Nd isotope data

reported for another Udachnaya-East groundmass sample (Pearson et al., 1995).

PIPE AGE

Prior to 1997, ages ranging from 389 to 335 Ma had been suggested for the Udachnaya pipes. This interpretation was based on Rb-Sr data for carbonates and phlogopites (Maslovskaja et al., 1983), U-Pb zircon ages for nearby diamondiferous kimberlites (Sobolev, 1984), stratigraphic relationships (Pearson et al., 1995), Sm-Nd mineral ages for eclogitic xenoliths (Snyder et al., 1993), and K-Ar data for clinopyroxene inclusions in Udachnaya diamonds (Burgess et al., 1992). Kinny et al. (1997) and Griffin et al. (1999) reported sensitive high-resolution ion-microprobe U-Pb perovskite ages of 367 ± 5 Ma (Udachnaya-East) and 361 ± 4 and 353 ± 5 Ma (Udachnaya-West), as well as similar perovskite ages (362–355 Ma) for other kimberlites in the Daldyn field.

In a Rb-Sr isochron plot (not shown), the data for bulk, L2, and residue of both samples define straight unmixing arrays that, if interpreted as isochrons, yield apparent ages of 351 ± 30 and 343 ± 20 Ma; pooling all six data points yields 347 ± 6 Ma (mean square of weighted deviates [MSWD] = 12, 0.7049 ± 0.0002). This apparent age is not changed if a small correction is applied to the L2 Rb/Sr ratios to account for possible leaching artifacts, i.e., excess of Rb in L1. The large salt aggregate (Fig. 2) with Rb-Sr characteristics reminiscent of mica yields a model age near 350 Ma for all likely initial $^{87}Sr/^{86}Sr$ values. Regression of the halite data with those for the bulk-L2-residue triples from both samples produces ages of 346 ± 2 Ma. Very similar

TABLE 1. RB-SR, SM-ND, AND U-PB ISOTOPE RESULTS FOR UDACHNAYA-EAST KIMBERLITE GROUNDMASS SAMPLES

	bulk	res	YBK-0 L1	L1*	L2	bulk	res	YBK-3 L1	L2	salt
Rb ppm	88.0	110.2	232.7		10.99	85.21	93.9	183.5	69.2	93.3
Sr ppm	1122	64.4	146.7		4375	933	55.4	226.4	3137	1.207
$^{87}Rb/^{86}Sr$	0.227	4.951	4.587		0.0073	0.265	4.92	2.347	0.064	250.7
$^{87}Sr/^{86}Sr$	0.70588	0.72956	0.70698		0.70496	0.70626	0.72907	0.70756	0.70538	1.94046
$^{87}Sr/^{86}Sr_i$	0.70469	0.70369	<0.700		0.70492	0.70488	0.70336	<0.700	0.70505	
Sm ppm	10.57	12.77		0.15	2.45	11.58	10.52		1.04	
Nd ppm	79.85	98.56		0.65	12.22	80.62	82.11		5.51	
$^{147}Sm/^{144}Nd$	0.0800	0.0783		0.1278	0.1212	0.0869	0.0775		0.1143	
$^{143}Nd/^{144}Nd$	0.512561	0.512591		0.512628	0.512618	0.512596	0.512568		0.512585	
$^{143}Nd/^{144}Nd_i$	0.512369	0.512403		0.512321	0.512327	0.512387	0.512382		0.512311	
εNd_i	+4.0	+4.6		+3.0	+3.2	+4.3	+4.2		+2.8	
U ppm	3.32	4.52		0.041	0.275	2.37	3.78		0.112	<0.01
Pb ppm	2.97	2.69		1.083	3.80	4.39	12.57		7.49	22.89
$^{238}U/^{204}Pb$	82.1	134.9		2.405	4.64	37.1	19.9		0.96	<0.001
$^{232}Th/^{204}Pb$	356	484		12.2	19.2	158	96		0.9	<0.01
$^{206}Pb/^{204}Pb$	23.533	26.442		18.833	19.249	20.867	19.942		18.905	18.795
$^{207}Pb/^{204}Pb$	15.794	15.946		15.540	15.566	15.645	15.594		15.544	15.530
$^{208}Pb/^{204}Pb$	44.983	49.442		38.437	38.583	41.812	40.302		38.545	38.513
$^{206}Pb/^{204}Pb_i$	18.71	18.55		18.69	18.98	18.70	18.77		18.85	18.79
$^{207}Pb/^{204}Pb_i$	15.53	15.52		15.53	15.55	15.53	15.53		15.54	15.53
$^{208}Pb/^{204}Pb_i$	38.5	40.6		38.2	38.2	38.9	38.6		38.5	38.5

Note: Bulk = unleached chips of kimberlite groundmass, L1 = water leachate, L2 = cold 1M HCl leachate, res = 1M HCl residue; YBK-0 L1* is a separate L1 water leachate analyzed for Sm-Nd and U-Pb. $^{87}Sr/^{86}Sr$ and $^{143}Nd/^{144}Nd$ ratios adjusted to SRM987 = 0.71023 and La Jolla = 0.511860. Initial Sr-Nd isotope ratios calculated for an age of 367 Ma. External precision (2 std. dev.) for ^{206}Pb, ^{207}Pb, $^{208}PB/^{204}Pb \approx \pm0.03\%$. Elemental concentrations by isotope dilution, Th by inductively coupled plasma-mass spectrometer (ICP-MS). Th/Pb for bulk fractions derived from (Th/U) × (U/Pb), with Th/U from ICP-MS and U/Pb from isotope dilution. Absolute 2σ errors for initial Pb isotope ratios, based on estimated uncertainties in U/Pb, Th/Pb, and Pb isotope ratios (1%, 2%, 0.03%), are ≤0.07, ≤0.01, and ≤0.24 for $^{206}Pb/^{204}Pb$, $^{207}Pb/^{204}Pb$, and $^{208}Pb/^{204}Pb$, respectively. Initial $^{208}Pb/^{204}Pb$ for YBK-0 res is probably an artifact. Further details of analytical techniques are given in Appendix DR1 (see footnote 1 in text).

apparent ages are obtained from U-Pb isotope unmixing arrays for the same fractions: 347 ± 2 (MSWD = 0.047, YBK-0) and 342 ± 2 (MSWD = 0.65, YBK-3). U-Pb data for the salt aggregate do not change these apparent ages. The significance of these ca. 347 Ma ages is unclear in view of the ca. 20 Ma older perovskite U-Pb age for the Udachnaya pipes. However, given the absence of alteration (which makes a ca. 347 Ma metasomatic alteration event seem unlikely) and possible weaknesses in the U-Pb perovskite data (high common Pb contents, total 14 ± 10 Ma range in reported ages for the two Udachnaya pipes; Kinny et al., 1997; Griffin et al., 1999), we consider our ca. 347 Ma age (with a likely nominal error of ±5 Ma) a plausible alternative estimate of the pipe age.

MANTLE ORIGIN OF CHLORIDES AND CARBONATES IN KIMBERLITE

Overall, the isotope data for both the silicate-rich residues and the soluble components (which collectively comprise the groundmass) fall within the field defined by most group I kimberlites from several cratons (Fig. 3), including those from Yakutia (Kostrovitskii et al., 2004). This conclusion does not change if our ca. 347 Ma age rather than the 367 Ma perovskite age (Kinny et al., 1997) is used for age corrections; a switch to the younger age merely produces more homogeneous Sr and Pb initial isotope ratios while barely changing the ε_{Nd} values. Although the data (corrected to 367 Ma) show some minor isotopic disequilibrium (Fig. 3), there is no

obvious evidence for a crustal contribution to the Cl-rich soluble groundmass components.

Crustal contributions could have come in the form of host rock–derived brines that form pools at the mine site. These brines are high in Mg, alkalies, and Cl and resemble typical cratonic shield brines (Fritz and Frape, 1982). Three brine samples with Sr concentrations near 1000 ppm show a narrow range in $^{87}Sr/^{86}Sr$ (0.70885–0.70897). This is higher than present-day $^{87}Sr/^{86}Sr$ ratios in Cl-rich water extracts from the kimberlite groundmass (L1, <0.707). Furthermore, the brines have very low Rb/Sr ratios (~0.01) compared to the L1 fractions (>0.8). The mine site brines, or similar fluids present in the past, are thus unlikely to have contributed Cl-rich soluble components to the kimberlite. This assertion is also supported by the 347 Ma Rb-Sr age for the salt aggregate in YBK-3; this chloride is clearly old and unrelated to recent alteration.

Formation waters from the Cambrian carbonate and evaporite sequences traversed by the pipe during emplacement could be another source of crustal contamination. However, our isotope data for L1* and the salt aggregate rule out a significant contribution from this source. Initial Pb isotope ratios in the salt aggregate and in the L1* leachate are almost identical to those of the silicate and carbonate fractions of the kimberlite groundmass (Table 1), implying a comagmatic origin. The same conclusion can be drawn from the high ε_{Nd} value (+3) in L1*. Furthermore, even the present-day $^{87}Sr/^{86}Sr$ ratios of the Cl-rich groundmass water leachates are lower than

those of the Cambrian carbonate-platform sequences of Siberia (0.7082–0.7088; Derry et al., 1994), implying that synmagmatic or post-magmatic contamination with fluids derived from these sequences is also unlikely. A similar argument applies to synmagmatic or post-magmatic contamination by Cl-rich fluids derived from the Cambrian evaporites. The $^{87}Sr/^{86}Sr$ ratios of the Cambrian evaporites were presumably similar to ambient seawater (0.7082–0.7088), or higher because of Sr import from surrounding cratonic areas. Radiogenic ingrowth since the Cambrian would have further raised the $^{87}Sr/^{86}Sr$ ratio. Any alteration fluids from the evaporites at any time would thus have $^{87}Sr/^{86}Sr$ far exceeding that in the kimberlite groundmass chlorides (<0.707).

In the absence of a plausible crustal source for the groundmass chlorides and carbonates and given the similar Nd and Pb isotope ratios in the water-soluble component and the silicate fraction of the groundmass, we conclude that the unusual groundmass chlorides and alkali carbonates in the Udachnaya-East pipe kimberlite must be mantle derived (Kamenetsky et al., 2004). This evidence, in combination with other observations, e.g., the presence of Cl-bearing inclusions in diamonds (Bulanova et al., 1998; Izraeli et al., 2001), and the strong effects of chlorides on diamond nucleation in carbonate fluids (Tomlinson et al., 2004), suggest a significant role of volatiles, in particular chlorine, in deep-mantle processes.
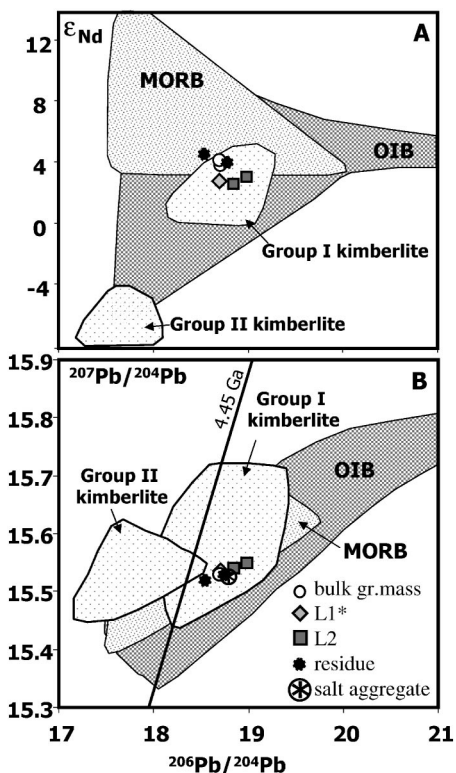
Figure 3. Initial isotope compositions, calculated at 367 Ma. A: $^{206}Pb/^{204}Pb$ vs ε_{Nd}. L1* water leachate plots close to points for unleached kimberlite groundmass (bulk) and silicate-rich residues, and all points plot within or close to field for kimberlites from several cratons with isotopic signatures similar to South African group I kimberlites (note that combined Pb and Nd isotope data are reported for only few cases). B: Pb isotope diagram. Note close coincidence of points for water leachate L1*, large salt aggregate (Fig. 2), and unleached (bulk) and leached groundmass samples (points for L1* and bulk groundmass overlap). Use of 347 Ma rather than 367 Ma age correction would result in reduced dispersion of data, with little change in absolute position. Fields for global group I and group II kimberlites, modern mid-oceanic-ridge basalt (MORB), and oceanic island basalt (OIB) are also shown. 4.45 Ga geochron is for reference only.

REFERENCES CITED

Alibert, C., and Albarède, F., 1988, Relationships between mineralogical, chemical, and isotopic properties of some North American kimberlites: Journal of Geophysical Research, v. 93, p. 7643–7671.

Bulanova, G.P., Griffin, W.J., and Ryan, C.G., 1998, Nucleation environment of diamonds from Yakutian kimberlites: Mineralogical Magazine, v. 62, p. 409–419.

Burgess, R., Turner, G., and Harris, J.W., 1992, $^{40}Ar-^{39}Ar$ laser probe studies of clinopyroxene inclusions in eclogitic diamonds: Geochimica et Cosmochimica Acta, v. 56, p. 389–402.

Dawson, J.B., 1980, Kimberlites and their xenoliths: New York, Springer, 252 p.

Derry, L.A., Brasier, M.D., Corfield, R.M., Rozanov, A.Y., and Zhuravlev, A.Y., 1994, Sr and C isotopes in Lower Cambrian carbonates from the Siberian craton: A paleoenvironmental record during the "Cambrian explosion": Earth and Planetary Science Letters, v. 128, p. 671–681.

Fritz, P., and Frape, S.K., 1982, Saline groundwaters in the Canadian Shield: A first overview: Chemical Geology, v. 36, p. 179–190.

Golovin, A.V., Sharygin, V.V., Pokhilenko, L.N., Mal'kovets, V.G., Kolesov, B.A., and Sobolev, N.V., 2003, Secondary melt inclusions in olivine from unaltered kimberlites of the Udachnaya-East pipe, Yakutia: Doklady Earth Sciences, v. 388, p. 93–96.

Griffin, W.L., Ryan, C.G., Kaminsky, F.V., O'Reilly, S.Y., Natapov, L.M., Win, T.T., Kinny, P.D., and Ilupin, I.P., 1999, The Siberian lithosphere traverse: Mantle terranes and the assembly of the Siberian craton: Tectonophysics, v. 310, p. 1–35.

Haggerty, S.E., 1999, A diamond trilogy: Superplumes, supercontinents, and supernovae: Science, v. 285, p. 851–860.

Harris, M., le Roex, A., and Class, C., 2004, Geochemistry of the Uintjiesberg kimberlite, South Africa: Petrogenesis of an off-craton, group I, kimberlite: Lithos, v. 74, p. 149–165.

Izraeli, E.S., Harris, J.W., and Navon, O., 2001, Brine inclusions in diamonds: A new upper mantle fluid: Earth and Planetary Science Letters, v. 187, p. 323–332.

Kamenetsky, M.B., Sobolev, A.V., Kamenetsky, V.S., Maas, R., Danyushevsky, L.V., Thomas, R., Sobolev, N.V., and Pokhilenko, N.P., 2004, Kimberlite melts rich in alkali chlorides and carbonates: A potent metasomatic agent in the mantle: Geology, v. 32, p. 845–848.

Kinny, P.D., Griffin, W.L., Heaman, L.M., Brakhfogel, F.F., and Spetsius, Z.V., 1997, SHRIMP U-Pb ages of perovskite from Yakutian kimberlites: Russian Geology and Geophysics, v. 38, p. 91–99.

Kostrovitskii, S.I., Morikiyo, T., Serov, I.V., and Rotman, A.Y., 2004, Origin of kimberlites: Evidence from isotopic-geochemical data: Doklady Earth Sciences, v. 399, p. 1164–1168.

le Roex, A.P., Bell, D.R., and Davis, P., 2003, Petrogenesis of group I kimberlites from Kimberley, South Africa: Evidence from bulk-rock geochemistry: Journal of Petrology, v. 44, p. 2261–2286.

Maslovskaja, M.H., Yegorov, K.N., Kolosnitsyna, T.I., and Brandt, S.B., 1983, Strontium isotope composition, Rb-Sr absolute age, and rare alkalies in micas from Yakutian kimberlites: Doklady Akademii Nauk SSSR, v. 266, p. 451–455.

Mitchell, R.H., 1986, Kimberlites: Mineralogy, geochemistry and petrology: New York, Plenum Press, 442 p.

Mitchell, R.H., 1989, Aspects of the petrology of kimberlites and lamproites: Some definitions and distinctions, in Ross, J., et al., eds., Kimberlites and related rocks: Their composition, occurrence, origin and emplacement, Volume 1: Sydney, Blackwell Scientific Publications, p. 7–45.

Pal'yanov, Y.N., Sokol, A.G., Borzdov, Y.M., and Khokhryakov, A.F., 2002, Fluid-bearing alkaline carbonate melts as the medium for the formation of diamonds in the Earth's mantle: An experimental study: Lithos, v. 60, p. 145–159.

Pavlov, D.I., and Ilupin, I.P., 1973, Halite in Yakutian kimberlite, its relations to serpentine and the source of its parent solutions: USSR Academy of Sciences Transactions, v. 213, p. 178–180.

Pearson, D.G., Snyder, G.A., Shirey, S.B., Taylor, L.A., Carlson, R.W., and Sobolev, N.V., 1995, Archaean Re-Os age for Siberian eclogites and constraints on Archaean tectonics: Nature, v. 374, p. 711–713.

Pelechaty, S.M., Grotzinger, J.P., Kashirtsev, V.A., and Zhernovsky, V.P., 1996, Chemostratigraphic and sequence stratigraphic constraints on Vendian–Cambrian basin dynamics, northeast Siberian craton: Journal of Geology, v. 104, p. 543–563.

Price, S.E., Russell, J.K., and Kopylova, M.G., 2000, Primitive magma from the Jericho pipe, NWT, Canada: Constraints on primary kimberlite melt chemistry: Journal of Petrology, v. 41, p. 789–808.

Rao, N.V.C., Gibson, S.A., Pyle, D.M., and Dickin, A.P., 2004, Petrogenesis of Proterozoic lamproites and kimberlites from the Cuddapah basin and Dharwar craton, southern India: Journal of Petrology, v. 45, p. 907–948.

Snyder, G.A., Jerde, E.A., Taylor, L.A., Halliday, A.N., Sobolev, V.N., and Sobolev, N.V., 1993, Nd and Sr isotopes from diamondiferous eclogites, Udachnaya kimberlite pipe, Yakutia, Siberia: Evidence of differentiation in the early Earth?: Earth and Planetary Science Letters, v. 118, p. 91–100.

Sobolev, N.V., 1984, Kimberlites of the Siberian platform: Their geological and mineralogical features, in Glover, J.E., and Harris, P.G., eds., Kimberlite occurrence and origin: A basis for conceptual models in exploration: Perth, University of Western Australia, p. 275–287.

Sun, S.-S., and McDonough, W.F., 1989, Chemical and isotopic systematics of oceanic basalts: Implications for mantle composition and processes, in Saunders, A.D., and Norry, M.J., eds., Magmatism in the ocean basins: Geological Society [London] Special Publication 42, p. 313–345.

Tomlinson, E., Jones, A., and Milledge, J., 2004, High-pressure experimental growth of diamond using C-K_2CO_3-KCl as an analogue for Cl-bearing carbonate fluid: Lithos, v. 77, p. 287–294.

1. GSA Data Repository item xxxxxx, Appendix TABLE. CHEMICAL COMPOSITIONS OF THE UDACHNAYA-EAST PIPE KIMBERLITE GROUNDMASS, LEACHATE AND RESIDUE SAMPLES

	YBK-0 bulk-gm	YBK-1 bulk-gm	YBK-3 bulk-gm	res	YBK-0 L1	L2	res	YBK-3 L1	L2
SiO_2	27.06	26.08	25.24						
TiO_2	1.23	1.12	1.40	1.43*	0.02*	0.11*	1.34*	0.10*	0.02*
Al_2O_3	2.13	1.74	2.11						
FeO	7.63	7.16	6.92						
MnO	0.15	0.13	0.13	0.16*	0.0*	0.03*	0.17*	0.01*	0.02*
MgO	29.41	29.59	27.79	>10*	0.6*	2.79*	>10*	1.07*	1.93*
CaO	12.70	12.04	12.41						
Na_2O	3.47	4.33	5.06		2.15*			3.07*	
K_2O	1.85	2.17	2.23		0.79*			1.16*	
P_2O_5	0.49	0.42	0.41						
NiO	0.14	0.14	0.13						
Cr_2O_3	0.16	0.13	0.23						
CO_2	9.83	10.27	10.71		1.48[#]			2.34[#]	
H_2O	0.45	0.45	0.63						
Cl	2.24	2.97	3.11		2.31			3.28	
SO_3	0.55	0.67	0.82		0.53**			0.90**	
LOI	14.17	16.01	16.64						
Soluble part	7.30	9.67	10.77						
Li	13.9	12.2	13.3	19.1	27.7	7.6	20.2	3.6	5.0
Be	1.3	1.0	1.4	1.0	0.1	3.4	0.8	0.1	1.4
Cr	1167	1002	1755	2571	44	97	1667	57	25
Ni	1053	1102	995	1141	56	80	1559	26	63
Co	79	77	72	90	1.9	10.0	111	2.8	7.0
Cu	64	55	55	85	30.8	100	73	31.4	35.3
Zn	61	59	58	90	11.0	10.6	96	10.4	5.1
V	102	93	114	143	20.5	149	132	33.3	83
Sc	12.9	11.4	13.1	9.1	1.9	5.9	17.0	2.0	3.9
Mo	1.2	1.1	1.6	0.4	16.7	0.7	0.4	10.3	1.1
Sn	1.5	4.5	2.7	1.1	0.4	0.4	1.0	0.6	0.3
Sb	0.1	0.1	0.2	0.2	0.3	0.2	0.2	0.2	0.1
Cs	0.9	1.0	1.1	0.8	3.0	1.2	0.7	2.6	1.0
Ba	1130	1173	1211	2071	140	1179	1717	293	413
Ga	5.6	4.7	5.2	8.8	0.4	3.5	7.8	0.9	1.2
Rb	73	85	86	109	245	43	95	185	34
Sr	892	838	897	65	156	4257	57	225	3222
Y	10.2	7.7	7.7	8.6	0.7	20.1	7.8	1.3	7.8
Zr	115	98	101	172	5.3	45	164	19.7	9.8
Nb	153	131	139	273	3.7	27.3	241	24.8	3.4
La	97	81	75	151	3.1	59	130	11.8	19.0
Ce	167	140	129	270	4.0	65	240	19.8	18.0
Pr	17.5	14.7	13.5	28.2	0.4	5.8	25.3	1.9	1.5
Nd	58	49	45	97.5	1.3	20.1	88.2	6.8	5.3
Sm	7.8	6.5	6.0	12.6	0.2	3.5	11.1	1.1	1.0

Eu	2.0	1.7	1.6	3.2	0.1	1.2	2.8	0.3	0.4
Gd	4.9	4.0	3.8	7.5	0.2	3.5	6.5	0.7	1.3
Tb	0.6	0.5	0.4	0.8	n.d.	0.5	0.7	0.1	0.2
Dy	2.5	2.0	1.9	3.4	0.1	3.1	2.9	0.4	1.0
Ho	0.4	0.3	0.3	0.5	n.d.	0.6	0.4	n.d.	0.2
Er	0.9	0.7	0.7	1.1	0.1	1.5	1.0	0.1	0.6
Tm	0.1	0.1	0.1	0.1	n.d.	0.2	0.1	n.d.	0.1
Yb	0.6	0.4	0.5	0.5	n.d.	1.1	0.5	0.1	0.3
Lu	0.1	0.1	0.1	0.1	n.d.	0.1	0.1	n.d.	0.1
Hf	2.5	2.2	2.3	3.9	0.1	0.6	3.6	0.3	0.1
Ta	8.2	7.1	8.2	16.3	0.1	0.1	13.4	1.1	n.d.
Pb	3.5	5.3	7.0	2.5	0.5	3.6	11.8	1.9	7.5
Th	11.7	10.7	9.1	15.7	0.2	1.1	17.5	0.3	0.1
U	2.8	4.2	2.2	4.3	0.1	1.2	3.7	0.4	0.2

Note: Major element data for bulk groundmass (bulk gm) samples by XRF on fused discs; trace element data by solution-mode ICPMS. Data for Na, K, etc. for water leachates (L1) determined by Analytical Services of Tasmania (see Analytical Methods); Data for Mg, Ti and Mn for L1 by ICPMS solution. L1 = water leachates; L2 = 1M HCl leachates; res = residues from 1M HCl leach. * - weight percent of element, #-CO_3, **-SO_4, n.d. - not determined.

2. GSA Data Repository item xxxxxx, Details of Analytical Methods

Sample preparation: Internal groundmass fragments (<1 mm) from fresh kimberlite were handpicked with carefully cleaned new steel and plastic tools to avoid contamination of fragment surfaces. This was necessary because the principal aim of this work was to chemically and isotopically characterize water-soluble alkali-chloride and alkali-carbonate components in the groundmass. These components were to be extracted using a leach with cold distilled water. In contrast to most other isotopic studies, this meant that the sample fragments could not be cleaned to remove laboratory contamination at any stage prior to isotopic analyses. In order to gauge the likely extent of contamination, a Pb-Sr blank was determined for the stainless steel spatula used to remove parts of the salt segregation (Fig.2). This was done by collecting repeated dilute HCl rinses from the tip of the (previously acid cleaned) spatula. This "smear" blank, representing ≈ 2 cm^2 of the spatula's surface, contained ≈ 0.3 ng of Pb, with a $^{206}Pb/^{204}Pb$ near 17, and ≈ 30 pg of Sr. As only the very tip of the spatula, with an area of ≈ 0.5 cm^2, came in contact with the sample, the contribution from "smear" blank is unlikely to exceed 100 pg of Pb and 10 pg of Sr. These blank levels are small compared to the total amount of Pb and Sr within the analysed salt sample (≈ 240 ng Pb, 20.5 ng Sr).

Leaching, sample dissolution and aliquotting: Separates of groundmass fragments weighing ≈ 100 mg were leached with (1) cold distilled water, for 20 minutes, followed by (2) cold 1M HCl. After each leach step, leachates were pipetted off, combined with a water rinse, and the respective residues were dried and re-weighed to determine mass loss. The HCl-residues ("res"), as well as separate samples of unleached "bulk" groundmass, were dissolved with HF-HNO_3 (48 hrs) and 6M HCl (12 hrs) in Krogh-type high-pressure bombs in an oven set at 160°C. The sample solutions were then split for separate analysis of (i) trace elements, (ii) U-Pb isotope

dilution, (iii) Pb isotope composition, and (iv) Sm-Nd and Rb-Sr isotopes. The water leachates (L1) were analysed for trace elements and Rb-Sr isotopes; U-Pb and Sm-Nd isotope data were obtained on a separate water leach for sample YBK-0 ("L1*") after trace element data for L1 indicated Pb-Nd levels sufficient for isotopic work. The ca. 12 x 5 mm salt segregation found in YBK-3 (Fig.2) was dissolved in cold water and, following determination of approximate trace element contents on a small test aliquot, was split for separate determination of (i) U-Pb isotope dilution, (ii) Pb isotopic composition, (iii) Rb-Sr isotope dilution, and (iv) Sr isotopic composition.

Chemical and isotopic analyses: Major and trace element compositions of three groundmass samples, including YBK-0 and YBK-3, and trace elements in L1, L2 and res fractions, were determined at the University of Tasmania, by fused disc XRF and solution-mode ICP-MS, respectively (Yu et al., 2001). Major cation and anion contents in water leachates were measured by Analytical Services Tasmania, using ICP-AES for cations, and ion chromatography with electronic suppression and conductivity detection (Dionex DX100) for anions. Carbon was determined using a Carlo Erba CHNS-O elemental analyzer at the University of Tasmania. Selected trace and major element data were plotted on a standard multi-element diagram after normalization to primitive mantle values of Sun and McDonough, 1989.

Samples for isotopic analysis were spiked with mixed ^{235}U-^{208}Pb, $^{87 \text{ or } 85}$Rb-^{84}Sr and ^{149}Sm-^{150}Nd spikes as required, and prepared for mass spectrometry using a combination of conventional cation exchange and EICHROM^{TM} resin methods (Pin et al., 1994; Pin and Zalduegui, 1997; Theriault and Davis, 1999). Dissolution and chemistry blanks were measured on numerous occasions and always remained below 50 pg (Sm-Nd, Rb-Sr, U) and 100 pg (Pb, highest blanks associated with bomb dissolutions).

All isotopic analyses were done on a NU Instruments multi-collector ICP-MS at the University of Melbourne using methods adapted from several sources (Vance and Thirlwall, 2002; Waight et al., 2002a; Waight et al., 2002b; Woodhead, 2002). Simultaneous corrections for mass bias and spike in Sr and Nd isotope analyses were done on-line using an iterative algorithm. Kr interference (ca. 3 mV at 83Kr) from impurities in the Ar gas was largely removed by the on-peak-zero correction routine. Small residual Kr interferences related to drift in the Kr signal during the run were removed by a conventional isobar correction based on the 83Kr monitor isotope; the 86Kr/83Kr and 84Kr/83Kr ratios used were those measured on pure Kr background prior to introduction of Sr (i.e. with 88Sr at baseline) at the start of a Sr session. Strontium isotope data were normalized to ^{86}Sr/^{88}Sr=0.1194 and are reported relative to SRM987=0.71023. Results for the E&A Sr carbonate standard and spiked USGS standards BCR-1 and BHVO-1 adjusted the same way yielded ^{87}Sr/^{86}Sr ratios of 0.708005±47, 0.705016±46 and 0.703478±36, respectively (all errors are external precision, 2sd). ^{84}Sr/^{86}Sr ratios in unspiked Sr averages 0.05648±3. Nd isotope data were normalized to ^{146}Nd/^{145}Nd=2.0719425 (equivalent to ^{146}Nd/^{144}Nd = 0.7219) and are reported relative to La Jolla Nd = 0.511860. Adjusted results for Nd standard JNd$_i$-1 average 0.512113±22, BCR-1 yields ^{147}Sm/^{144}Nd = 0.1380±2 and ^{143}Nd/^{144}Nd = 0.512641±18, while BHVO-1 yields 0.1493±3 and 0.512998±18. Our data for standards compare well with TIMS Sr-Nd isotope data for these standards (e.g., Raczek et al., 2003; Tanaka et al., 2000). CHUR parameters are 0.1967 and 0.512638. Mass bias in Pb isotope analyses is corrected using a variant of the Tl-doping method (Woodhead, 2002). Under routine conditions, this method provides an external precision (2sd) of 0.02-0.03% for ^{206,207,208}Pb/^{204}Pb. Errors for U/Pb are <±1%. Age corrections were done for an age of 367 Ma. Absolute 2σerrors for initial Pb isotope

ratios, based on estimated uncertainties in U/Pb, Th/Pb and Pb isotopic ratios (1%, 2%, 0.03%), are ≤ 0.07, ≤ 0.01, ≤ 0.24 for $^{206}Pb/^{204}Pb$, $^{207}Pb/^{204}Pb$ and $^{208}Pb/^{204}Pb$, respectively. High initial $^{208}Pb/^{204}Pb$ for YBK-0 res is probably an artifact. Decay constants are: ^{87}Rb 1.42×10^{-11}/yr; ^{147}Sm 6.54×10^{-12}/yr; ^{238}U 0.155125×10^{-9}/yr; ^{235}U 0.98485×10^{-9}/yr; ^{232}Th 0.049485×10^{-9}/yr.

Pin, C., Briot, D., Bassin, C., and Poitrasson, F., 1994, Concomitant separation of strontium and samarium -neodymium for isotopic analysis in silicate samples, based on specific extraction chromatography: Analytica Chimica Acta, v. 298, p. 209-217.

Pin, C., and Zalduegui, J.F.S., 1997, Sequential separation of light rare-earth elements, thorium and uranium by miniaturized extraction chromatography: application to isotopic analyses of silicate rocks: Analytica Chimica Acta, v. 339, p. 79-89.

Raczek, I., Jochum, K.P., and Hofmann, A.W., 2003, Neodymium and strontium isotope data for USGS reference materials BCR-1, BCR-2, BHVO-1, BHVO-2, AGV-1, AGV-2F GSP-1, GSP-2 and eight MPI-DING reference glasses: Geostandards Newsletter-the Journal of Geostandards and Geoanalysis, v. 27, p. 173-179.

Sun, S.-S., and McDonough, W.F., 1989, Chemical and isotopic systematics of oceanic basalts: implications for mantle composition and processes, *in* Saunders, A.D., and Norry, M.J., eds., Magmatism in the Ocean Basins, Volume 42: London, Geological Society Special Publication, p. 313-345.

Tanaka, T., Togashi, S., Kamioka, H., Amakawa, H., Kagami, H., Hamamoto, T., Yuhara, M., Orihashi, Y., Yoneda, S., Shimizu, H., Kunimaru, T., Takahashi, K., Yanagi, T., Nakano, T., Fujimaki, H., Shinjo, R., Asahara, Y., Tanimizu, M., and Dragusanu, C., 2000, JNdi-1: a neodymium isotopic reference in consistency with LaJolla neodymium: Chemical Geology, v. 168, p. 279-281.

Theriault, R.J., and Davis, W.J., 1999, Rapid extraction of Sr and Pb by ion-specific chromatography for thermal ionisation mass spectrometry analysis, Radiogenic age and isotopic studies, Volume Report 12, Geological Survey of Canada, Current Research, p. 9-12.

Vance, D., and Thirlwall, M., 2002, An assessment of mass discrimination in MC-ICPMS using Nd isotopes: Chemical Geology, v. 185, p. 227-240.

Waight, T., Baker, J., and Peate, D., 2002a, Sr isotope ratio measurements by double-focusing MC-ICPMS: techniques, observations and pitfalls: International Journal of Mass Spectrometry, v. 221, p. 229-244.

Waight, T., Baker, J., and Willigers, B., 2002b, Rb isotope dilution analyses by MC-ICPMS using Zr to correct for mass fractionation: towards improved Rb-Sr geochronology?: Chemical Geology, v. 186, p. 99-116.

Woodhead, J., 2002, A simple method for obtaining highly accurate Pb isotope data by MC-ICP-MS: Journal of Analytical Atomic Spectrometry, v. 17, p. 1381-1385.

Yu, Z., Robinson, P., and McGoldrick, P.J., 2001, An evaluation of methods for the chemical decomposition of geological materials for trace element analysis using ICP-MS: Geostandards Newsletter-the Journal of Geostandards and Geoanalysis, v. 25, p. 199-217.